An Associative Mechanism for Reductive Elimination of d^8 $NiR_2(PR_3)_2$

Kazuyuki Tatsumi,*† Akira Nakamura,*† Sanshiro Komiya,‡ Akio Yamamoto,§ and Takakazu Yamamoto§

Contribution from the Department of Macromolecular Science, Faculty of Science, Osaka University, Toyonaka, Osaka 560, Japan, the Department of Applied Chemistry for Resources, Tokyo University of Agriculture & Technology, Nakamachi, Koganei, Tokyo 184, Japan, and the Research Laboratory of Resources Utilization, Tokyo Insitutute of Technology, Nagatsuta, Midori-ku, Yokohama 227, Japan. *Received February 21, 1984*

Abstract: Addition of neutral ligands to d^8 *cis*-MR_2L_2 has been known to promote reductive elimination of R–R for some Ni(II) complexes. A molecular orbital analysis of the reaction is presented to show how the fifth ligand affects the elimination step. The study led us to explore complex polytopal rearrangements of the five-coordinate intermediates. Liberation of R–R was found to proceed easily from the *cis*-dialkyl SP structure **1**, the entry point of an association process from *cis*-NiR_2L_2, and from the nearby TBP structure **5**. The other cis isomers are unstable, or the elimination from there is symmetry forbidden, and *trans*-NiR_2L_2 finds no favorable pathway to give reductive elimination products. We also discuss the effects of donor or acceptor strength of an incoming ligand upon the reaction.

Formation of carbon–carbon bonds is always an attractive synthetic prospect. Especially common in such transition-metal-catalyzed reactions is the coupling of two coordinated alkyl groups into an alkane, which proceeds for a great variety of metals.[1] Among others, the mechanism of the reductive elimination from d^8 metal alkyls has been relatively well envisaged because of its experimental tractability.

Let us briefly review what is known about reductive eliminations, making references only to those of square-planar d^8 dialkyls. These are summarized in Scheme I. Direct elimination of R–R from the four-coordinate species is rather rare and occurs in a few *cis*-dialkylnickel(II),[2,1a,1s] hydridoalkylplatinum(II),[1o] and diarylplatinum(II) complexes only.[1i] For Pd(II)[3] and Au(III)[4,9] there emerged kinetic evidence for elimination from a three-coordinate intermediate.[5,6] Another intriguing point is that liberation of R–R via the dissociative mechanism takes place clearly from *cis*-MR_2L_2 but never from *trans*-MR_2L_2.[7] This signifies that T-shaped *trans*-MR_2L, which might be produced by freeing L from *trans*-MR_2L_2, will encounter a substantial energy barrier to rearrangement to *cis*-MR_2L.[8] The theoretical analyses based on the extended-Hückel calculations have corroborated these features of the dissociative mechanism.[9,10]

On the other hand, addition of netural ligands to MR_2L_2 has been found to promote reductive elimination in some Ni(II) cases, by way of five-coordinate intermediates. For example, the cleavage of Ni–R bonds in NiR_2(bipy) is facilitated through coordination of olefins with electronegative substituents.[1a] Also known are acceleration effects of added phosphine ligands on thermolysis of $NiCH_3(C_6H_4X)$(dmpe), which leads to the facile elimination of CH_3–C_6H_4X.[11] Again *trans*-NiR_2L_2 isomers were found not to give elimination products in this associative mechanism [1r] (Scheme II).

Following the earlier work on the reactions of four- and three-coordinate dialkyls,[10] we are interested in building an understanding of reactions of five-coordinate complexes. In this theoretical contribution, our goal is to gain an insight into the detailed mode of the reaction and to provide some discrimination among mechanistic alternatives differing in pentacoordination geometry. We will also attempt to answer the puzzling question: why do *trans*-dialkyls not undergo elimination although the trans five-coordinate intermediates appear to undergo trans–cis isomerization along normally facile Berry pseudorotation pathways? The case is special, but the theoretical analysis lends itself to obvious extention to understand some key steps in a broad range of organometallic reactions. Our analysis was carried out by means of extended-Hückel calculations, with parameters listed in Appendix I.

Scheme I

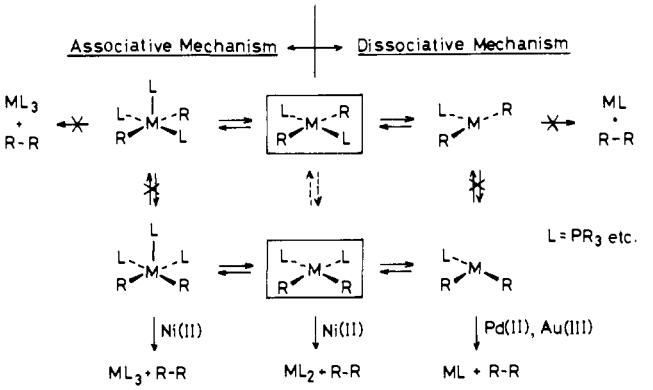

Scheme II

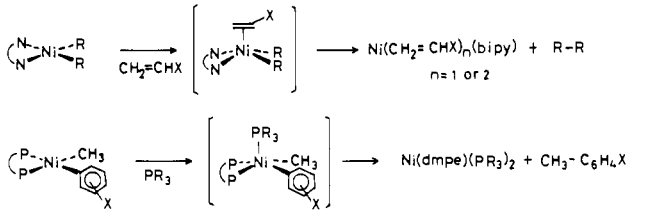

(1) (a) Yamamoto, T.; Yamamoto, A.; Ikeda, S. *J. Am. Chem. Soc.* **1971**, *93*, 3350–3359. (b) Latyaeva, V. N.; Razuvaev, G. A.; Malisheva, A. V.; Kiljakova, G. A. *J. Organomet. Chem.* **1964**, *2*, 388–397. (c) Razuvaev, G. A.; Latyaeva, V. N.; Vishinskaya, L. I.; Rabinovitch, A. M. *Ibid.* **1973**, *49*, 441–444. (d) Coates, G. E.; Parkin, C. *J. Chem. Soc.* **1963**, 421–429. (e) Davidson, P. J.; Lappert, M. F. *J. Chem. Soc., Chem. Commun.* **1973**, 317. (f) Johnson, A.; Puddephatt, R. J. *J. Organomet. Chem.* **1975**, *85*, 115–121. (g) Shaw, C. F., III; Lundeen, J. W.; Tobias, R. S. *Ibid.* **1973**, *51*, 365–374. (h) Brown, M. P.; Puddephatt, R. J.; Upton, C. E. *Ibid.* **1973**, *49*, C61–C63; *J. Chem. Soc., Dalton Trans.* **1974**, 2457–2465. (i) Braterman, P. S.; Cross, R. J.; Yong, G. B. *J. Chem. Soc., Dalton Trans.* **1976**, 1306–1309, 1310–1314. (j) Ruddick, J. D.; Shaw, B. L. *J.* Chem. *Soc. A* **1969**, 2969–2970. (k) Clark, H. C.; Manzer, L. E. *Inorg. Chem.* **1973**, *12*, 362–368. (l) Appleton, T. G.; Clark, H. C.; Manzer, L. E. *J. Organomet. Chem.* **1974**, *65*, 275–287. (m) Davidson, P. J.; Lappert, M. F.; Pearce, R. *Chem. Rev.* **1976**, *76*, 219–242 and references therein. (n) Schrock, R. R.; Parshall, G. W. *Ibid.* **1976**, *76*, 243–268 and references therein. (o) Abis, L.; Sen, A.; Halpern, J. *J. Am. Chem. Soc.* **1978**, *100*, 2915–2916 and references therein. (p) Norton, J. R. *Acc. Chem. Res.* **1979**, *12*, 139–145 and references therein. (q) Ertl, J.; Debaerdemaeker, T.; Brune, H. A. *Chem. Ber.* **1982**, *115*, 3860–3874. (r) Smith, G.; Kochi, J. K. *J. Organomet. Chem.* **1980**, *198*, 199–214. (s) Kohara, T.; Yamamoto, T.; Yamamoto, A. *J. Organomet. Chem.* **1980**, *192*, 265–274.

† Osaka University.
‡ Tokyo University of Agriculture & Technology.
§ Tokyo Institute of Technology.

0002-7863/84/1506-8181$01.50/0

Scheme III

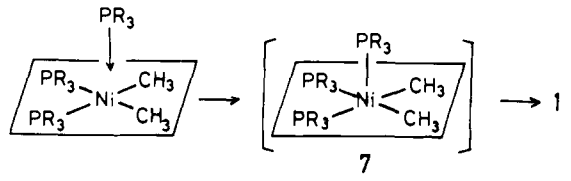

Reductive Elimination from Cis Five-Coordinate Nickel(II) Dialkyls. Given the stoichiometry $Ni(CH_3)_2(PR_3)_3$, the five-coordinate intermediate has various possible isomers, from some of which the reductive elimination of CH_3–CH_3 may proceed. Imposing the requirement of either a square-pyramidal (SP) or trigonal-bipyramidal (TBP) framework, we have six limiting geometries, as shown in structures **1**–**6**. An addition of phosphine

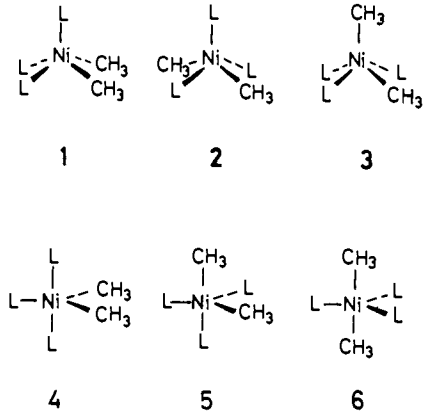

to a square-planar *cis*-$Ni(CH_3)_2(PR_3)_2$ initiates the associative mechanism. The phosphine is likely to approach Ni from the direction perpendicular to the molecular plane to give the entry point into the five-coordinate manifold. Thus the immediate product should assume an SP structure **1** (Scheme III), and our first concern is the elimination from this geometry.

It is pedagogically more useful, however, to consider a hypothetical structure, **7** beforehand, for we want to compare the reaction with those of three- and four-coordinate species. **7** is similar to **1**, but retains the planarity of the $Ni(CH_3)_2(PR_3)_2$ portion. To make our interpretation clearer, our analysis will be mostly on $Ni(CH_3)_2A_3^{3-}$ with the hydride-model ligand A^- which replaces PR_3. Hereafter we will omit the molecular charge from the formula of the model complexes in the text. A is a hydrogen atom whose 1s orbital is set equal to the calculated energy of a lone pair (−14.34 eV) of a model phosphine, PH_3. The choice of ligand is of course important, in the sense that stronger donor ligands, being trans to the leaving groups, give a higher barrier for the elimination reaction.[10] The essence has something to do with their σ donor or acceptor strength, and the phosphine ligands in the actual Ni complexes have little π-bonding capability if any.

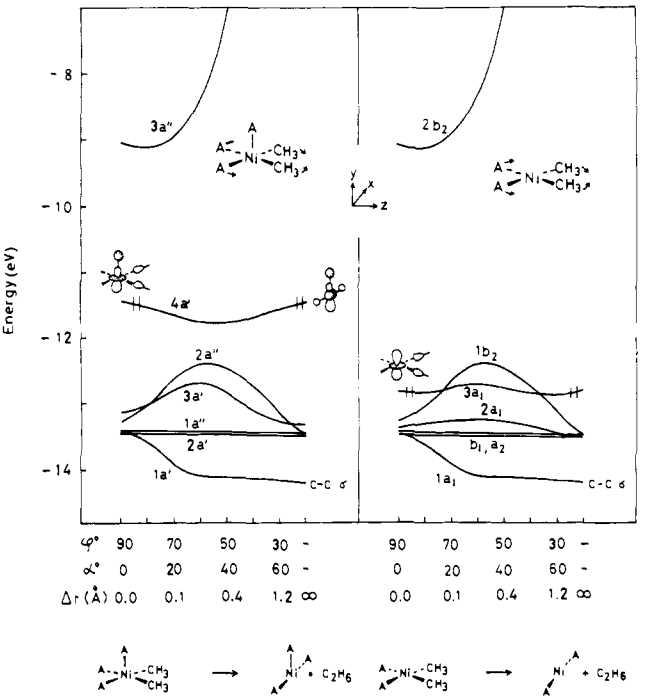

Figure 1. Evolution of energy levels for elimination of C_2H_6 from square-pyramidal $Ni(CH_3)_2A_3$ (left) and square-planar $Ni(CH_3)_2A_2$ (right). The reaction coordinate is specified at bottom where the variational parameters are defined in **8**, **9**, and **10**.

The primitive reaction coordinate we employ here has evolved in the studies of Hoffmann's group.[9,10] Three degrees of freedom are varied simultaneously as are defined in **8**: C–Ni–C angle φ,

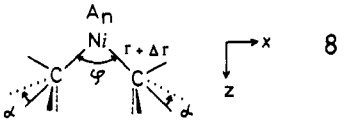

the rocking angle α between the local threefold axis of the methyl group and the Ni–C bond line, and the stretching of Ni–C Δr from $r = 2.02$ Å. An additional degree of freedom, a relaxation of the NiA_n remnant to its preferred geometry, must also be taken into account. For $n = 2$, i.e., the reaction from the four-coordinate molecule, we incorporated into our reaction coordinate the opening up of the AMA angle θ as two methyls depart (**9**). While the

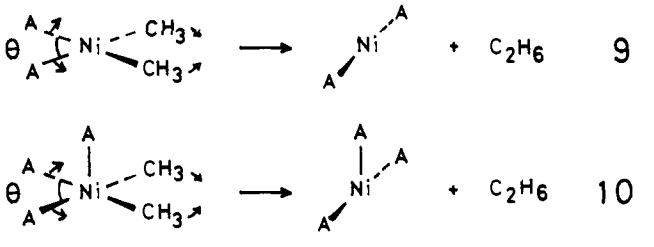

assumed coordinate is greatly simplified, the geometry of the transition state in the path was found very similar to the one obtained by the recent rigorous calculations.[12] For the elimination from **7**, we first allow the NiA_3 fragment to rearrange to a T shape by unbending the two in-plane Ni–A bonds (**10**).

(2) (a) Grubbs, R. H.; Miyashita, A.; Liu, M.; Burk, P. *J. Am. Chem. Soc.* **1977**, *99*, 3863–3864; *Ibid.* **1978**, *100*, 2418–2425. (b) Grubbs, R. H.; Miyashita, A. *Ibid.* **1978**, *100*, 1300–1302, 7416–7418, 7418–7420.

(3) (a) Ozawa, F.; Ito, T.; Nakamura, Y.; Yamamoto, A. *Bull. Chem. Soc. Jpn.* **1981**, *54*, 1868–1856. (b) Milstein, D.; Stille, J. K. *J. Am. Chem. Soc.* **1979**, *101*, 4981–4991. (c) Gillie, A.; Stille, J. K. *Ibid.* **1980**, *102*, 4933–4941.

(4) (a) Tamaki, A.; Magennis, S. A.; Kochi, J. K. *J. Am. Chem. Soc.* **1974**, *96*, 6140–6148. (b) Tamaki, A.; Kochi, J. K. *J. Organomet. Chem.* **1972**, *40*, C81–C84; **1973**, *51*, C39–C42.

(5) Reductive eliminations from some Pt(II) and Pd(II) complexes occur after oxidative addition of an RX, thus via d^6 M(IV) six- and five-coordinate intermediates. (a) See ref 1h and 1j–1l. (b) Loar, M. K.; Stille, J. K. *J. Am. Chem. Soc.* **1981**, *103*, 4174–4181. (c) Moravskiy, A.; Stille, J. K. *Ibid.* **1981**, *103*, 4182–4186.

(6) A mechanism was proposed in which reductive elimination of Ni(II) complexes was promoted by prior electron-transfer processes. Morrell, D. G.; Kochi, J. K. *J. Am. Chem. Soc.* **1975**, *97*, 7262–7270.

(7) Ozawa, F.; Ito, T.; Yamamoto, A. *J. Am. Chem. Soc.* **1980**, *102*, 6457–6463 and references therein.

(8) Although cis–trans isomerization between two T-shaped geometries is a high-energy process, a similar swing motion of poor donor ligand L in d^8 MR_2L is facile. See ref 10 and McCarthy, T. J.; Nuzzo, R. G.; Whitesides, G. M. *J. Am. Chem. Soc.* **1981**, *103*, 1676–1678.

(9) Komiya, S.; Albright, T. A.; Hoffmann, R.; Kochi, J. K. *J. Am. Chem. Soc.* **1976**, *98*, 7255–7265; **1977**, *99*, 8440–8447.

(10) Tatsumi, K.; Hoffmann, R.; Yamamoto, A.; Stille, J. K. *Bull. Chem. Soc. Jpn.* **1981**, *54*, 1857–1867.

(11) Komiya, S.; Abe, Y.; Yamamoto, A.; Yamamoto, T. *Organometallics* **1983**, *2*, 1466–1468.

(12) Blomberg, M. R. A.; Brandemark, U.; Siegbahn, P. E. J. *J. Am. Chem. Soc.* **1983**, *105*, 5557–5563.

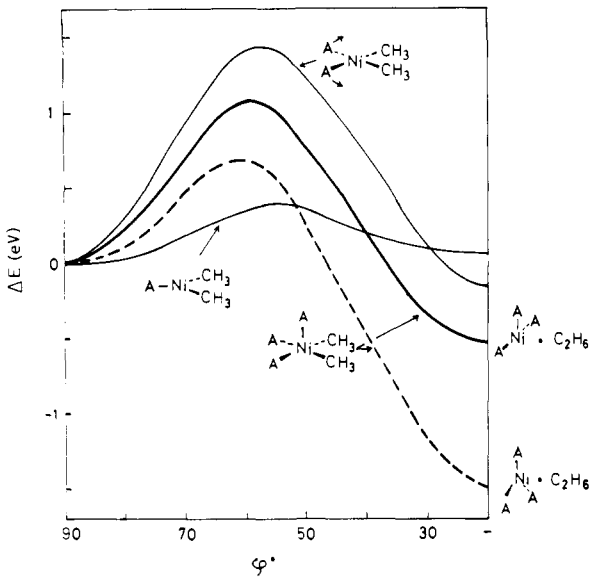

Figure 2. Total energy curves for elimination of C_2H_6 from $Ni(CH_3)_2A$, $Ni(CH_3)_2A_2$, and $Ni(CH_3)_2A_3$. The dashed line curve is for the reaction of $Ni(CH_3)_2A_3$, where the NiA_3 portion is relaxed to a trigonal-planar structure as shown in **14**. The reaction coordinate is the same as the one specified in detail at the bottom of Figure 1.

Figure 1 shows the evolution of the energy levels along such a reaction coordinate for $Ni(CH_3)_2A_3$. As a comparison, the orbital diagram for **9** is also given. Both **9** and **10** are symmetry allowed; i.e., no costly level crossing occurs between occupied and unoccupied orbitals.[13,14] In our previous paper, the activation barrier to the elimination from d^8 cis-four-coordinate complexes was attributed to the $1a_1$–$1b_2$ differential, and as usual the higher orbital $1b_2$ dominated.[10] This hold true of **9**. The $1b_2$ of $Ni(CH_3)_2A_2$ consists of a bonding assemblage of Ni d_{xz} and methyl lone pairs with Ni p_x mixing in. Or $1b_2$ can be regarded as an out-of-phase combination of the two Ni–CH_3 bond orbitals, while $1a_1$ is the in-phase counterpart. The other orbitals, i.e., b_1,a_2, $2a_1$,$3a_1$, and high-lying $2b_2$, are formally Ni d levels, representing the familiar four-below-one splitting pattern for square-planar ML_4 complexes. The $1b_2$ and $1a_1$ orbitals develop into a pure Ni d_{xz} **11** of the linear NiA_2 and the CH_3–CH_3 σ orbital **12**, respectively, as the reaction proceeds.

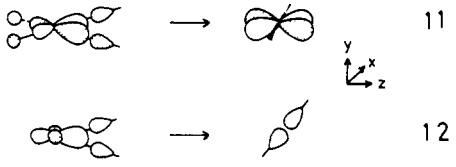

11

12

The addition of an axial σ ligand does not perturb the b_2 orbitals of $Ni(CH_3)_2A_2$ at all. Only the assignment is changed to 2a″ and 3a″ in the lower C_s symmetry of $Ni(CH_3)_2A_3$. On the other hand, the fifth ligand reorganizes the a_1 orbitals in a complicated way. The most significant outcome is destabilization of one a_1 orbital, being 4a′ in Figure 1 left.

The solid lines in Figure 2 give the total energy profiles for **9** and **10**, together with the one for elimination from a Y-shaped three-coordinate species, $Ni(CH_3)_2A$. All curves are referred to an arbitrary zero of energy at $\varphi = 90°$, $\alpha = 0°$, and $\Delta r = 0.0$ Å.

(13) Other theoretical studies on reductive elininations: (a) Pearson, R. G. *Acc. Chem. Res.* **1971**, *4*, 152–160; "*Symmetry Rules for Chemical Reactions*"; Wiley-Interscience: New York, **1976**; pp 286, 405. (b) Braterman, P. S.; Cross, R. J. *Chem. Soc. Rev.* **1973**, *2*, 271–294. (c) Åkermark, B.; Ljungqvist, A. *J. Organomet. Chem.* **1979**, *182*, 59–75. (d) Åkermark, B.; Johansen, H.; Roos, B.; Wahlgren, U. *J. Am. Chem. Soc.* **1979**, *101*, 5876–5883. (e) Balazs, A. C.; Johnson, K. H.; Whitesides, G. M. *Inorg. Chem.* **1982**, *21*, 2162–2174. (f) Flores-Riveros, A.; Novaro, O. *J. Organomet. Chem.* **1982**, *235*, 383–393.

(14) Theoretical work on the Grubbs system is available. Mckinney, R. J.; Thorn, D. L.; Hoffmann, R.; Stockis, A. *J. Am. Chem. Soc.* **1981**, *103*, 2595–2603.

The electronic origin of the small energy barrier (0.4 eV) for $Ni(CH_3)_2A$ was already examined in detail.[10] Suffice it to mention that the $1b_2$ orbital of $Ni(CH_3)_2A$ does not rise as sharply as that of $Ni(CH_3)_2A_2$ as the reaction approaches the transition state. The computed barrier for $Ni(CH_3)_2A_2$ amounts to 1.4 eV.

Interestingly **10** gives a barrier 0.4 eV smaller than **9**, though it is not as low as the one obtained for $Ni(CH_3)_2A$. As can be seen in Figure 1, 2a″ provides the large part of the barrier for **10**, like $1b_2$ does for **9**. However, the explanation for the difference between **9** and **10** cannot rely on these orbitals because they behave in exactly the same fashion along the reaction coordinate. 1a″ (or a_2) and 2a′ (or b_1) are innocent concerning the barrier. Then the rest, 1a′ + 3a′ + 4a′ vs. $1a_1 + 2a_1 + 3a_1$, should be and actually are responsible for the distinction. As noted earlier, however, the reorganization of the a_1 symmetry orbitals of $Ni(CH_3)_2A_2$ by the addition of an axial ligand is complicated, and we are unable to point to any particular one of them as a primal cause.

Pursuing another line of strategy we show in **13** how the overlap populations between Ni and surrounding ligands evolve along **9** and **10**. The sum of overlap populations $\sum P$ is given at the bottom of each structure. The overlap-population changes $\Delta(\sum P)$ reflect in principle the amount of loss or gain of Ni–ligand bond energies. Since we do not count the C–C overlap population of the ethane product in the summation, $\Delta(\sum P)$ is calculated to be negative. It is evident that $\sum P$ decreases more in **13b** than in **13a**. The

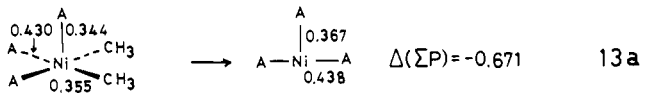

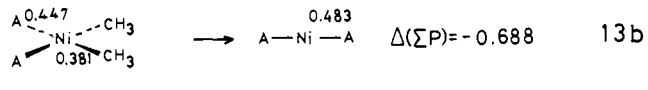

main cause of this trend comes from the larger Ni–CH_3 overlap population of the four-coordinate reactant $Ni(CH_3)_2A_2$. Thus the elimination from $Ni(CH_3)_2A_2$ costs Ni–ligand bond energies more than the reaction of $Ni(CH_3)_2A_3$, indicating that the reaction **13b** requires more energy to proceed. This conclusion based on the population analysis is confirmed by the potential energy curves in Figure 2. The stability of the product relative to the reactant is lesser for $Ni(CH_3)_2A_2$ and the trend is kept over the transition-state region. To put it in other words, the Ni–CH_3 overlap population of $Ni(CH_3)_2A_3$ is smaller than that of $Ni(CH_3)_2A_2$, indicating that liberation of the methyl groups occurs more easily from the five-coordinate species. We should note here again that the calculated difference arises from the congeries of contribution from each a_1 (or a′) orbital and not from $1b_2$ (or 2a″).

The difference between the Ni–CH_3 overlap populations in $Ni(CH_3)_2A_3$ and $Ni(CH_3)_2A_2$ is caused by the way in which the Ni 4s orbital participates in the Ni–CH_3 bonds. For $Ni(CH_3)_2A_2$, Ni 4s can hybridize with d_{y^2} and reduces the antibonding between the filled d_{y^2} and methyl lone pairs, primarily in the $3a_1$ molecular orbital of Figure 1 right. On the other hand, this favorable hybridization is hampered by the presence of the axial ligand in $Ni(CH_3)_2A_3$. The Ni 4s–d_{y^2} mixing is now well set up for minimizing the d_{y^2}–A(axial) antibonding and is not as effective at doing so for the Ni–CH_3 bonds as the corresponding mixing in $Ni(CH_3)_2A_2$. This effect is partly seen in the partial overlap populations calculated between Ni 4s and CH_3, which are 0.128 for $Ni(CH_3)_2A_3$ and 0.140 for $Ni(CH_3)_2A_2$.

The above observations fit the bulk of the associative mechanism proposed for reductive eliminations in question. They are predicted upon the principle of the well-known LFER theory and sound sensible in that addition of an extra ligand facilitates the succeeding elimination step. Interestingly, the electronic factor which favors the associative mechanism contrasts with the electronic factor found in explaining the dissociative mechanism. The small reductive elimination barrier in three-coordinate complexes was

referred to the low $1b_2$ level in energy at a transition state relative to the $1b_2$ of four-coordinate complexes in our previous paper.[10] Thermodynamically the dissociative mechanism should be (and is) disadvantageous, because the elimination from the three-coordinate species results in formation of an unstable one-coordinate molecule, NiA. We may say that this mechanism becomes feasible due to the "kinetically controlled" factor. On the other hand, the associative mechanism can be termed "thermodynamically controlled".

We deepen our analysis of $Ni(CH_3)_2A_3$. Obviously the T-shape structure is not the stable conformation of d^{10} NiA_3, and the relaxation to a T-shape **10** is by no means the best choice of reaction pathways. The favorable NiA_3 structure is trigonal planar (D_{3h}), and the stability relative to the T-shape was calculated to be 0.97 eV. We now relax the NiA_3 part to D_{3h} by moving the two basal A atoms down as shown in **14**. Then D_{3h} NiA_3 sits

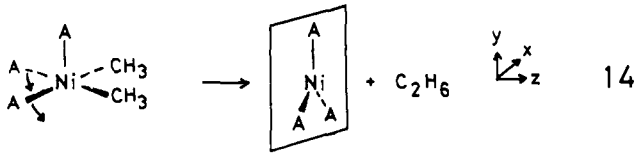

14

in the xy plane at the end of reaction. The potential energy curve along the new reaction coordinate is plotted by a broken line in Figure 2. The LFER theory is again at work. Enhanced stability of the dissociation product lowers the activation barrier by 0.4 eV compared with that for **10**. The decrease in barrier makes the elimination more advantageous than direct elimination from the four-coordinate complexes.

When examining the reaction from $Ni(CH_3)_2A_3$ of the SP structure **1**, we were obliged to optimize the geometry. This was done by varyir the angle between apical and basal bonds, φ as defined in **15**. The calculated minimum comes at $\varphi = 101°$ which

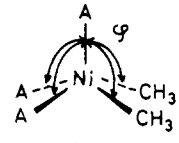

15

is 0.48 eV more stable than $\varphi = 90°$. This minimum will correspond to circled a in Figure 4, and to the structure **17a**. The C–Ni–C angle in the optimized geometry is no longer 90°, but is still close to it (87.9°). Then our handy reaction coordinate **8** (and a relaxation pathway similar to **14** for the NiA_3 portion) was utilized in estimating the activation energy for elimination from the square-pyramidal minimum. The dotted curve in Figure 3 shows the result, and the barrier is now 1.0 eV. The energy curve for **14** is given again by a broken line in the figure as a template. The activation energy is higher than that for **14**, simply because the reaction starts at a more stable conformation. However, it remains well below the barrier obtained for $Ni(CH_3)_2A_2$. And the essence of our analysis based on the "pedagogical" pathways, **10**, as well as **14**, holds. Consequently the associative mechanism gains a firmer footing.

Of the six SP and TBP structures, **1** was found to be a possible exit channel for elimination of CH_3–CH_3. Apparently elimination could proceed also from **3**, **4**, and **5**, for they have methyls at adjacent positions like **1** does. We now examine this possibility. The relative stabilites of these cis geometries were calculated by varying two parameters φ_1 and φ_2 independently from 90° to 130° in **16a** and **16b**. φ_1 describes the synchronous bending of a trans

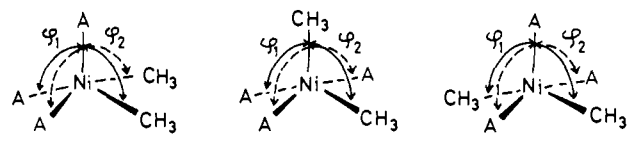

16a 16b 16c

pair of the equatorial ligands, while φ_2 is for the other trans pair.

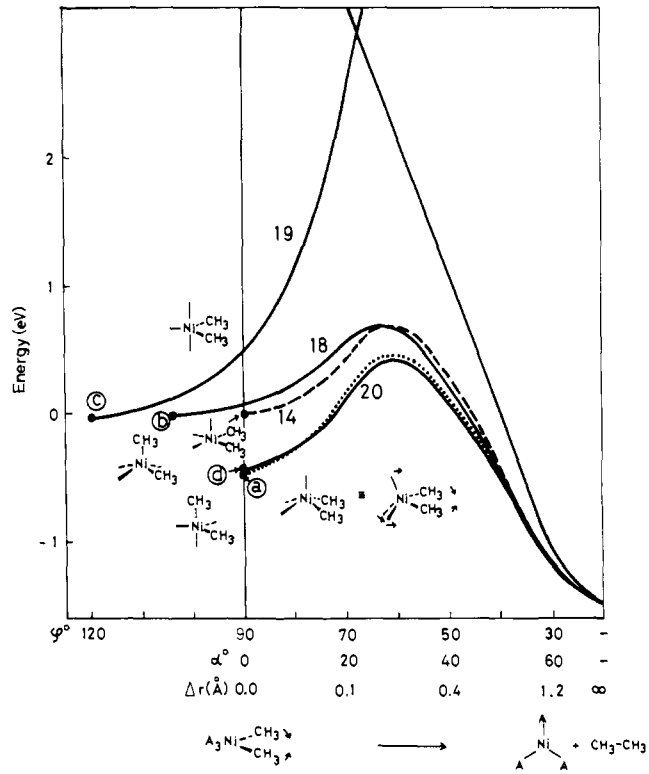

Figure 3. Total energy curves for elimination of C_2H_6 from various structures of $Ni(CH_3)_2A_3$. The model A ligands sit at the unmarked sites of the structures. The NiA_3 portion of all the structures is relaxed to a trigonal-planar form at the end of the reaction. When the reaction starts at the point in which the CH_3–Ni–CH_3 angle φ is greater than 90°, we allowed the molecules to reduce the angle φ down to 90° first. In the region, $90° \geq \varphi \geq 0°$, the reaction coordinate for the leaving CH_3 groups is the same as the one shown at the bottom of Figure 1. The dashed line curve is for the reaction **14**, which is given also in Figure 2. The minuscules enclosed with a circle correspond to those defined in **17a–c** and in Figure 4. The numbers by the curves indicate the reaction pathways defined in the text. The reaction pathway for the dotted curve is shown in the figure, in which the reaction starts at the geometry **17a**.

The potential energy surfaces **16a** and **16b** approximately compass all the cis geometries in question. For example, **16b** can be either **3**, **4**, or **5** depending on the choice of φ_1 and φ_2. We have also calculated the potential energy surface for **16c**, which covers trans structures. This surface may not aid us at present, but will be necessary for a complete description of the five-coordinate intermediates in the next section. Figure 4 summarizes these three surfaces.

In Figure 4, we indicate by filled circles our choices of geometries which represent the $Ni(CH_3)_2A_3$ isomers. The SP structures are defined at the potential minima with the restriction of $\varphi_1 = \varphi_2$. On the other hand, we use standardized forms for TBP, where interligand angles in the equatorial plane are 120°. They are not always at local potential minima in the surfaces, but are convenient pivoting points in the successive Berry pseudorotation processes which will be discussed shortly. The relative stabilities of the six isomers were calculated to be in the order **17f > 17a ~17d > 17e > 17c ~ 17b**. The energies shown below the structures are relative to an energy zero at $\varphi_1 = 90°$ and $\varphi_2 = 125°$. Note that these ideal structures are not necessarily at local minima. Electronic reasons for the stability trend can be traced to the difference in σ-donor capability between CH_3 and A (or PR_3). Namely, a stronger donor, CH_3 in this case, tends to occupy a basal position in SP or an axial site of TBP in d^8 complexes. For a detailed analysis of the site preference, readers should refer to the comprehensive study of ML_5 complexes by Rossi and Hoffmann.[16]

(15) (a) Klein, H. F.; Karsch, H. H. *Chem. Ber.* **1972**, *105*, 2628–2636. (b) Jeffery, E. A. *Aust. J. Chem.* **1973**, *26*, 219–220.

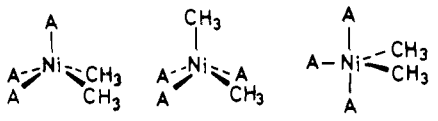

ΔE(eV)	0.038	0.498	0.460
	17a	**17b**	**17c**

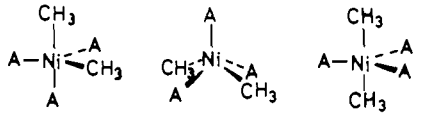

0.040	0.109	-0.066
17d	**17e**	**17f**

We now consider reductive elimination of two methyl groups from **17b**, **17c**, and **17d**. The reaction coordinates, i.e., the ways in which we relaxed the NiA_3 portion to the D_{3h} structure are illustrated in **18–20**. For **18** and **19**, the reaction starts at the

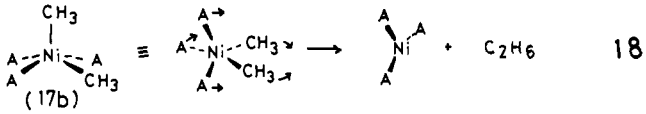

18

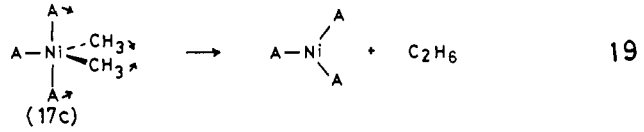

19

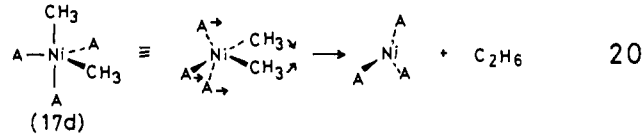

20

point in which the C–Ni–C angle is greater than 90°. Thus we allowed the molecules to reduce their C–Ni–C angles down to 90° first, keeping other geometries fixed, and then to follow our model reaction coordinate afterward. There is a distressing number of possible relaxation pathways and they are closely related to polytopal rearrangements of the five coordination geometries. We choose least motions which retain the shape of each starting geometry as much as possible. The reaction pathway **19** holds the C_{2v} symmetry and the others are C_s.

As can be seen in Figure 3, the potential energy curve for **20** is very like that obtained for the reaction of **17a**. Thus **17d** is able to eliminate alkane as easily as **17a**, although the net activation energy for **18** is lower than that for **20**. The energy at the transition state is higher than those of the above two reaction pathways.

An interesting aspect of Figure 3 is that the pathway **19** meets a prohibitively high barrier. The orbital correlation diagram in Figure 5 clearly tells that the reaction is symmetry forbidden. The $2b_2$ orbital, being occupied in the reactant **17c**, goes up sharply in energy and crosses with the unoccupied $3a_1$ as the reaction proceeds. $2b_2$ correlates to Ni p_x of NiA_3 and $3a_1$ moves down to become a occupied Ni d orbital. It should be pointed out that most of the reductive elimination reactions are symmetry allowed, and those of d^8 dialkyl complexes have so far confirmed this trend including three-, four-, and five-coordinate molecules.[10,13] The rare forbidden nature found for **19** should be kept in mind when one considers the associative mechanism for the d^8 species. One should also note that forbiddance of the reaction **19** is characteristic of d^8 complexes and that this reaction pathway becomes

(16) Rossi, A. R.; Hoffmann, R. *Inorg. Chem.* **1975**, *14*, 365–374.

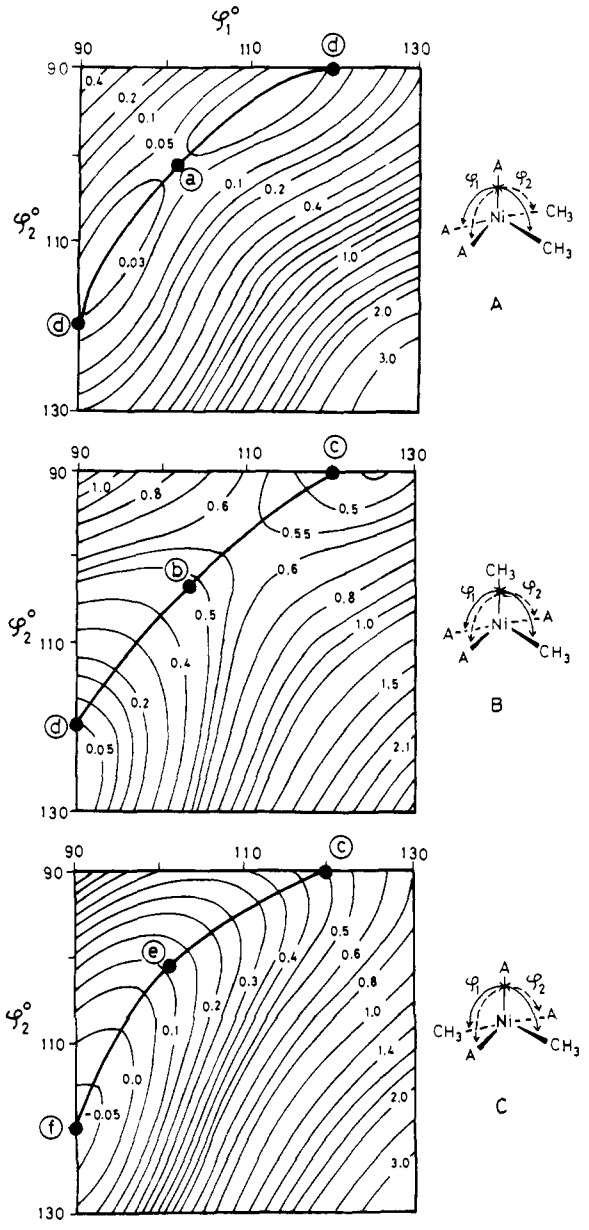

Figure 4. Potential energy surfaces for the deformation of $Ni(CH_3)_2A_3$. The parameter φ_1 describes the synchronous bending of a trans pair of the equatorial ligands, while φ_2 is for the other trans pair. The contours are in eV relative to an energy zero at $\varphi_1 = 90°$, $\varphi_2 = 125°$ of B. The filled circles indicate our choice of geometries of the $Ni(CH_3)_2A_3$ isomers. The encircled minuscules correspond to those defined in **17a–f**. Thick lines connecting the filled circles are Berry pseudorotation pathways.

symmetry allowed when two electrons are removed, thus for d^6 MR_2L_3.

***trans*- vs. *cis*-$Ni(CH_3)_2(PR_3)_2$ in the Associative Mechanism.** We have examined in detail how the associative mechanism works in case of *cis*-$NiR_2(PR_3)_2$. It is natural to think that the addition of phosphine occurs also to *trans*-$NiR_2(PR_3)_2$, yielding the five-coordinate trans-SP, **2**. The geometry does not have a direct channel open for an elimination step, because the two alkyls are still trans to each other. However, there remains a chance that it may find a bypass route to any one of the cis isomers through polytopal rearrangements, and eventually liberate alkane. From the experiments, we know that this does not happen. And let us explain why.

The bypass routes, if any, would be Berry pseudorotations. In Scheme IV, the six limiting structures are connected by three distinct pseudorotations. The unmarked sites contain phosphines. Coordination of a phosphine to *cis*-$NiR_2(PR_3)_2$ brings one into an SP-shaped entry point **1**, which is midway on the pseudorotation

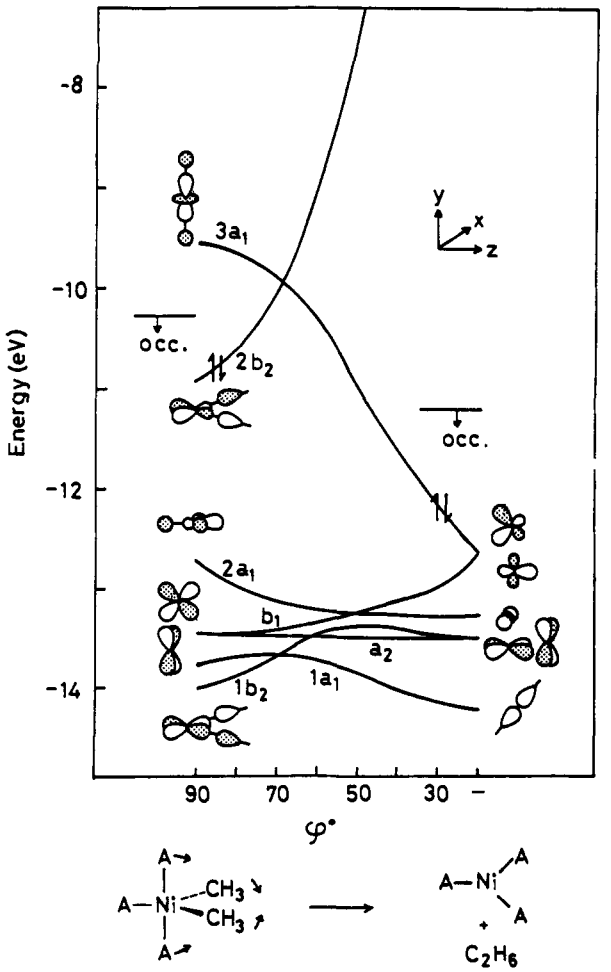

Figure 5. Evolution of energy levels along the pathway **19** for the elimination of C_2H_6. The reaction coordinate for the $Ni(CH_3)_2$ part is the same as the one given at the bottom of Figure 1.

Scheme IV

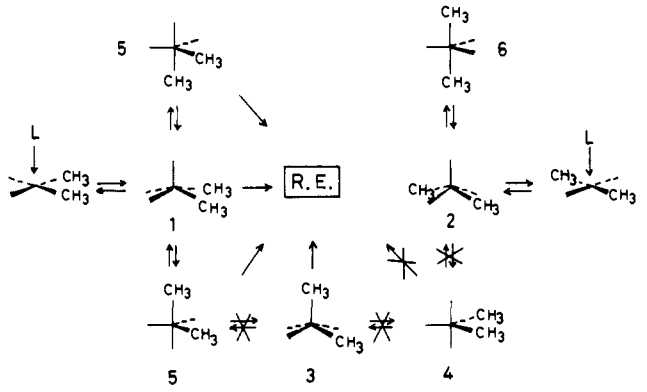

connecting two identical TBP forms, **5**. *trans*-$NiR_2(PR_3)_2$ enters into the five-coordination manifold at **2**. Obviously no direct pathway of isomerization is available between **1** and **2**, but they are topologically connected by another pseudorotation.

The potential energy surfaces in Figure 4, being calculated for the model compound $Ni(CH_3)_2A_3$, provide information about energetics of the isomerization steps. From Figure 4A, one can see that the rearrangement **17d** ⇄ **17a** ⇄ **17d** is a very easy process, with actually no barrier. On the contrary, the passage **17d** → **17b** → **17c** contains a high barrier in Figure 4B. The geometry **17b** is close to the potential maximum, and elimination from there is unlikely. The third pseudorotation (Figure 4C) is a down-hill process when it goes from **17c** to **17e** to **17f**. The immediate product **17e** from *trans*-$Ni(CH_3)_2A_2$ thus relaxes directly into **17f**, the most stable structure of $Ni(CH_3)_2A_3$.

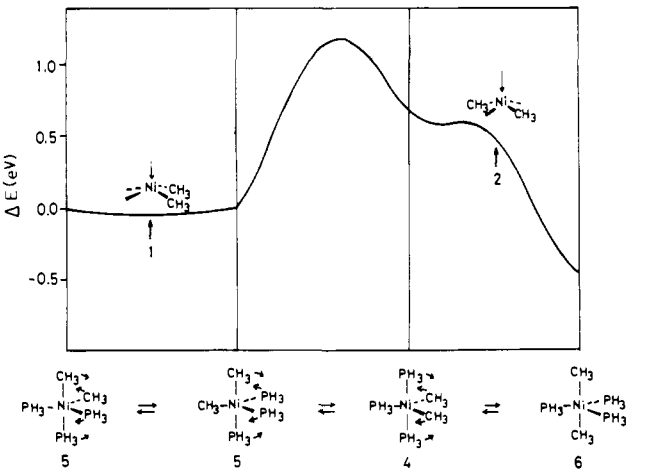

Figure 6. Potential energy curve for the successive Berry pseudorotations of $Ni(CH_3)_2(PH_3)_3$. The thick arrows below the curve indicate the entry points to the five-coordinate manifold by an addition of PH_3 to *cis*-$Ni(CH_3)_2(PH_3)_2$ (**1**) and *trans*-$Ni(CH_3)_2(PH_3)_2$ (**2**). The arrows in the structures at the bottom of the figure shows directions of the bending motions when the Berry processes occur from left to right.

Proceeding in the opposite direction toward **17c** requires energy, and even if the geometry is attained, elimination from it is symmetry forbidden. The energies of these pseudorotations will be compared with the barrier for the elimination reactions calculated for a realistic molecule, $Ni(CH_3)_2(PH_3)_3$.

Moving from the model $Ni(CH_3)_2A_3$ to a more realistic compound $Ni(CH_3)_2(PH_3)_3$ does not alter the conclusions concerning the Berry pseudorotations. Potential energy curves for the three different Berry processes of $Ni(CH_3)_2(PH_3)_3$ are assembled in Figure 6. The arrows indicate the entry points from cis and trans isomers of $Ni(CH_3)_2(PH_3)_2$. The calculated energy barrier between these points amounts to 1.2 eV from the cis side or 0.7 eV from the trans side. The barrier to the elimination of CH_3–CH_3 from $Ni(CH_3)_2(PH_3)_3$ of geometry **1**, i.e., the reaction similar to **14**, was calculated to be 0.2 eV. Furthermore, the entry point from *trans*-$Ni(CH_3)_2(PH_3)_2$ is at a sidehill of the potential curve which goes down to the most stable *trans*-dimethyl TBP structure, **6**. Thus, the cis and trans isomers are energetically shielded from each other. Any geometry in the Berry process between **1** and **5** can be an exit channel for reductive elimination, while **2** is likely to end up with the trans-TBP structure **6**.

The NMR studies for $Ni(CH_3)_2L_3$ (L = $P(CH_3)_3$, $P(CH_3)_2Ph$)[15] provide an excellent confirmation of the part of our conclusions. The stable structure of these molecules has been spectroscopically observed to be trigonal bipyramidal with two methyl groups at axial positions which is indeed at the potential minimum in our calculations.

Extensions. Electron-donor or -acceptor strength of an incoming ligand affects the ease of the elimination reaction. In unraveling the effect, it is convenient to divide the associative mechanism into the following three parts: (1) addition of the ligand L′ to square-planar $Ni(CH_3)_2(PR_3)_2$, (2) polytopal rearrangements of the adduct by the Berry mechanism, and (3) alkane elimination itself. As far as the first part is concerned, the trend is obvious. The weaker the σ electron-donor capability of the ligand L′ the more readily the addition takes place. This is because $Ni(CH_3)_2(PR_3)_2$ contains the occupied d_{z^2} orbital **21**, and the incoming ligand approaches from the direction of the orbital lobe.

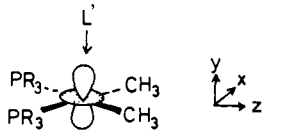

21

We are examining the case where the ligand L′ differs from PR_3. The five-coordinate adduct $Ni(CH_3)_2(PR_3)_2L'$ then gives

Scheme V

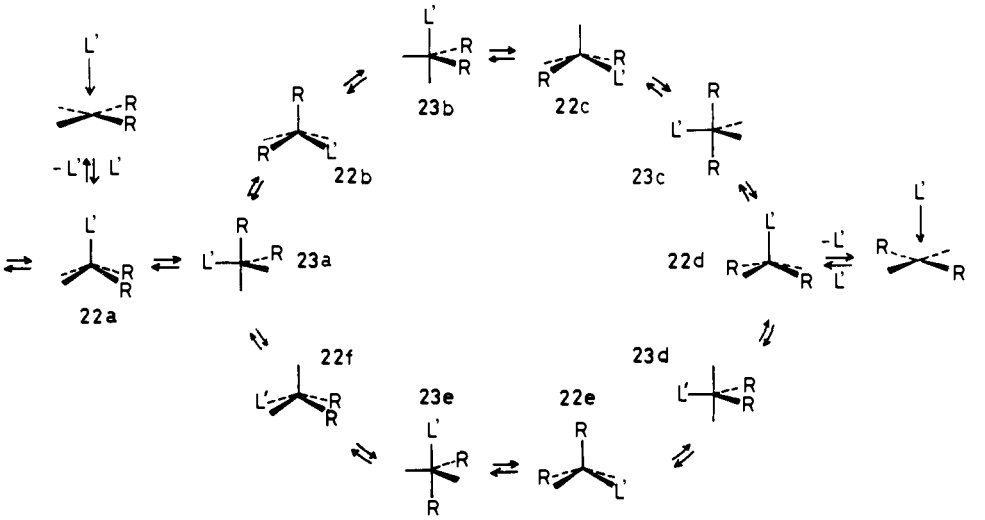

11 isomers (5 TBP, 6 SP), and these are topologically interrelated as shown in Scheme V. The relative stability of these isomeric structures as well as the ease of the elimination reaction from them depend on the choice of L′. The situation is complicated, but the reasonable degree of comprehension of these matters is available: Poorer σ-donors favor the apical sites of SP and the equatorial sites of TBP for d^8.[16] Also placing weaker σ-donors in the positions trans to the leaving alkyl groups facilitates the reductive elimination of R_2.[10]

Alkyl anions fall in the category of strong σ electron donors, and phosphines that sit at the unmarked sites in Scheme V are weak donors. When L′ is chosen to be a weak σ electron-donor, the most stable configurations of placing two alkyls in adjacent positions have to be again **22a** and **23a**. **22f** is probably stable too. The elimination of R_2 will then proceed from these structures. We showed in the early section that addition of phosphines (modeled by A) to *cis*-$Ni(CH_3)_2(PR_3)_2$ reduced the barrier for reductive elimination. In case that L′ is a weaker σ electron-donor than phosphines, the activation barrier could be reduced still more. If elimination occurs from **22a**, however, the effect is not great, because L′ stays nearly orthogonal to the plane in which dissociation of R–R proceeds. To probe this we performed a numerical experiment in which CH_3–CH_3 was eliminated from a hypothetical square-pyramidal structure of $Ni(CH_3)_2A_2A'$ via the pathway **14**. The *apical* ligand A′ is similar to our model ligand A but with a variable 1s orbital energy, $H_{ii}(A')$. The activation energy of **14** was reduced as $H_{ii}(A')$ was lowered, but very slightly, e.g., by only 0.01 eV on going from $H_{ii}(A') = -12.34$ to -14.34 eV, and by 0.02 eV from $H_{ii}(A') = -14.34$ to -16.34 eV. Reduction of the barrier should be much greater if the reaction takes place from the geometry **22f**, because the ligand A′ is now trans to a leaving alkyl group.[10]

The *trans*-dialkyl TBP geometry **23c** is probably the most stable of all. Either **22b** or **23b** in the upper portion of the Berry cycle, and either **22e** or **23d** in the lower portion are to be the least stable conformation. Whichever the case is, the cis–trans isomerization should meet a high barrier. The weaker the σ-donor strength of L′, the more pronounced is the geometrical preference for **22a**, **23a**, and **23c** over the above unstable conformers. Consequently the energy barrier to the cis–trans isomerization increases, as L′ lessens its σ-donor capability. The elimination becomes more difficult to take place from *trans*-$NiR_2(PR_3)_2$ under this condition.

What can be done to make the isomerization easier in the five-coordinate manifold? One way of doing this is to force the stable conformations **22a**, **23a**, and **23c** out of their potential wells. This can be achieved by introducing a good σ-donor for L′, and preferably better than R. Replacement of phosphines by potent σ-donors in the starting four-coordinate complexes should also help. However, such a substitution would result in an increment of the barrier to eliminating R–R.[10] Also a strong σ electron-donor L′ will not be easily added, thus making the associative mechanism less feasible. We are in a dilemma, or we should admit that facile reductive elimination via the associative mechanism and the cis–trans isomerization would not be accomplished at the same time.

There is experimental evidence that addition of $P(OEt)_3$ accelerates the reductive elimination of $NiR_2(PR_3)_2$ more than phosphines.[11] The order is $P(OEt)_3 > P(Et)_3 > P(aryl)_3 > P(Cy)_3$. We have to worry about the size of these ligands, because the approach toward $NiR_2(PR_3)_2$ is hampered by their steric bulkiness. Nevertheless, we think that the electronic factor, i.e., electron-withdrawing nature of $P(OEt)_3$, is operative in promoting the reaction. On the other hand, N-donors such as pyridine and triethylamine showed no acceleration effect. The extended-Hückel calculations show that the lone pair orbital of NH_3 is 0.59 eV higher in energy than PH_3. The stronger donor character of N-donors relative to P-donors could be a reason for the lack of acceleration effect.

Let us examine the case L′ = olefin[1a] which carries a π^* acceptor orbital. Scheme V is applicable, provided one sets the best orientation of olefin at each geometry. The orientational preference in d^8 TBP and SP has been established.[16,17] In a TBP structure, an equatorial olefin strongly favors a planar conformation, while a basal olefin in an SP has a powerful drive to stand upright. Assuming these, we calculated on $Ni(CH_3)_2(PH_3)_2(H_2C{=}CH_2)$ in the 11 geometrical variations. The *trans*-dialkyl TBP structure **24**, corresponding to **23c** in Scheme V, is again

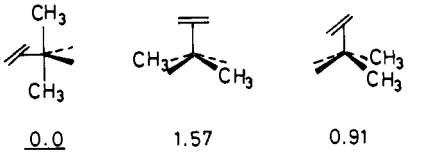

	24	**25**	**26**
ΔE(eV)	0.0	1.57	0.91

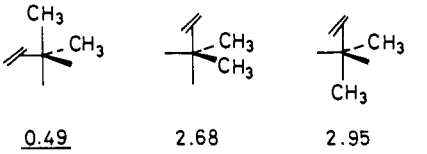

	27	**28**	**29**
	0.49	2.68	2.95

most stable. The geometry is 1.57 eV more stable than the trans entry point **25** (**22d** in Scheme V). The best cis isomer is another

(17) The orientational preference of olefin in five-coordinate d^4 complexes is opposite to the d^8 case. Kamata, M.; Hirotsu, K.; Higuchi, T.; Kido, M.; Tatsumi, K.; Yoshida, T.; Otsuka, S. *Inorg. Chem.* **1983**, *22*, 2416–2424.

Table I. Extended-Hückel Parameters

	orbital	H_{ii}, eV	exponent[a]
Ni	4s	-9.17	2.10
	4p	-5.15	2.10
	3d	-13.49	5.75 (0.5798) + 2.30 (0.5782)
P	3s	-18.6	1.60
	3p	-14.0	1.60
C	2s	-21.4	1.625
	2p	-11.4	1.625
H	1s	-13.6	1.3
A	1s	-14.34	1.3

[a] The d function is a double-ζ type.

TBP **27** (**23a**), to which the molecule relaxes from the nearby cis entry point, **26** (**22a**). The axial site of a TBP is not suited to ethylene, and **28** (**23b**) as well as **29** (**23e**) are unstable structures. There appear to be notable steric repulsions with the equatorial ligands, coupled with better back-bonding when the ethylene rotates back to an equatorial site. Stabilities of the other structures not listed in **24**-**29** fall in between those of **27** and **28**. The cis-trans rearrangements are again high-energy processes and unlikely to occur.[18]

The exit channel for R-R elimination might well be **23a**. The activation energy for the pathway **30** of the model $Ni(CH_3)_2(H_2C{=}CH_2)A_2$ was calculated to be 0.9 eV. The barrier is close to the one obtained for the pathway **14** of $Ni(CH_3)_2A_3$ (see Figure 3). One might anticipate that the barrier would be much lowered when A, and thus phosphine, is replaced by ethylene, because the strong π-accepting nature of ethylene stabilizes the three-coordinate product substantially. Presence of a π acceptor should also aid the alkane elimination itself. However, the calculated result opposes this naive expectation. Perhaps the π-acceptor effect is masked by the concomitant strong σ-donor character of ethylene. It has been known for experiments that addition of olefins facilitates reductive elimination, but only when electronegative substituents are attached to them.[1a]

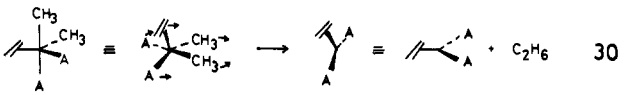

30

(18) It should be noted here that olefin insertion into M-R bonds, another ubiquitous reaction in organometallic chemistry, was found a difficult process for d^8 $PtXL_2(H_2C{=}CH_2)R$. Thorn, D. L.; Hoffmann, R. *J. Am. Chem. Soc.* **1978**, *100*, 2079-2089.

Appendix

The parameters of the extended-Hückel calculations[19] are listed in Table I. A weighted H_{ij} formula was used for calculations. Exponents of Ni 3d orbitals were taken from the work of Richardson et al.,[20] while other exponents and the H_{ij} values are the same as those used previously.[21]

Geometrical assumptions included the following: C—H 1.09 Å, C=C 1.34 Å, P—H 1.42 Å, Ni—$C(CH_3)$ 2.02 Å, Ni—(ethylene midpoint), 2.00 Å, Ni—P 2.23 Å, CH_3 and PH_3 tetrahedral.

Registry No. *trans*-$Ni(CH_3)_2(PH_3)_2$, 93219-79-5; *cis*-$Ni(CH_3)_2(PH_3)_2$, 79218-07-8.

(19) (a) Hoffmann, R. *J. Chem. Phys.* **1963**, *39*, 1397-1412. (b) Hoffmann, R.; Lipscomb, W. N. *Ibid.* **1962**, *36*, 2179-2189.
(20) Richardson, J. W.; Powell, R. R.; Nieuwpoort, W. C. *J. Chem. Phys.* **1963**, *38*, 796-801.
(21) Tatsumi, K.; Hoffmann, R. *J. Am. Chem. Soc.* **1981**, *103*, 3328-3341.

An Efficient Asymmetric Oxidation of Sulfides to Sulfoxides

P. Pitchen, E. Duñach, M. N. Deshmukh, and H. B. Kagan*

Contribution from the Laboratoire de Synthèse Asymétrique (associé au CNRS, UA 255), Université Paris-Sud, 91405 Orsay, France. *Received April 24, 1984*

Abstract: The Sharpless reagent for asymmetric epoxidation was modified by addition of 1 mol equiv of H_2O to give a new homogeneous reagent (Ti(O-*i*-Pr)$_4$/diethyl tartrate/H_2O/*t*-BuOOH = 1:2:1:1). This reagent cleanly oxidizes prochiral functionalized sulfides into optically active sulfoxides. The observed ee mainly ranged between 75 and 90% for alkyl aryl sulfoxides and 50-71% for dialkyl sulfoxides. A strong temperature dependence on ee was also observed in the asymmetric oxidation of methyl *p*-tolyl sulfoxide.

Chiral sulfoxides are gaining considerable importance in synthesis as chiral synthons for the asymmetric C-C bond formation.[1-4] Up to now, the main asymmetric synthesis of chiral sulfoxides has been based on the separation of the intermediate diastereomeric menthyl sulfinates.[5-8] Asymmetric oxidation of prochiral sulfides is not a preparative method for chiral sulfoxides:only moderate to high enantiomeric excesses have been observed in some cases.[9-14] We wish to present a simple method

(1) Mikolajczyk, M.; Drabowicz, J. *Top. Stereochem.* **1982**, *13*, 333.
(2) Solladié, G. *Synthesis* **1981**, 185.
(3) Posner, H. G.; Mallamo, J. P.; Miura, K.; Hulle, M. "Asymmetric Reactions and Processes in Chemistry"; American Chemical Society: Washington, DC, 1982; ACS Symp. Ser.
(4) (a) Corey, E. J.; Weigel, L. O.; Chamberlin, A. R.; Cho, H.; Hua, D. H. *J. Am. Chem. Soc.* **1980**, *102*, 6613. (b) Solladié, G.; Matloubi-Moghadam, F. *J. Org. Chem.* **1982**, *47*, 91.
(5) Andersen, K. K. *Tetrahedron Lett.* **1962**, 93.
(6) Mislow, K.; Green, M. M.; Laur, P.; Melillo, J. T.; Simmons, T.; Ternary, A. L., Jr. *J. Am. Chem. Soc.* **1965**, *87*, 1958.
(7) In some specific cases[2,8] procedures allow for recovery of only one diastereomer in epimerizing conditions at sulfur, by taking advantage of the greater stability or insolubility of one diastereoisomer.
(8) Mioskowski, C.; Solladié, G. *Tetrahedron Lett.* **1980**, *36*, 227.
(9) Oxidation by chiral peracids or oxaziridines (ee ≤30%): (a) Mayr, A.; Montanari, F.; Tramontini, D. *Gazz. Chim. Ital.* **1960**, *90*, 739. (b) Balenowic, K.; Bregant, N.; Francetti, D. *Tetrahedron Lett.* **1960**, 20. (c) Bucciarelli, F.; Forni, F.; Marcaccioli, S.; Moretti, I.; Torre, G. *Tetrahedron* **1983**, *39*, 187. (d) Davis, F. A.; Jenkins, R. H., Jr.; Awad, S. M.; Stringer, D. D.; Watson, W. H.; Galloy, J. *J. Am. Chem. Soc.* **1982**, *104*, 5412.
(10) Oxidation by other chemical reagents (ee <10%): (a) Higuchi, T.; Pitman, I. H.; Gensch, K. H. *J. Am. Chem. Soc.* **1966**, *88*, 5676. (b) Furia, F. D.; Modena, G.; Curci, R. *Tetrahedron Lett.* **1976**, 4637. (c) Liu, K. T.; Tong, Y. C. *J. Chem. Res. (S)* **1979**, 276.

0002-7863/84/1506-8188$01.50/0